Stabilization of Resistive Wall Modes by Magnetohydrodynamic Equilibrium Change Induced by Plasma Toroidal Rotation

J. Shiraishi[1], N. Aiba[2], N. Miyato[1] and M. Yagi[1]

[1]Japan Atomic Energy Agency, Rokkasho, Japan
[2]Japan Atomic Energy Agency, Naka, Japan

Corresponding Author: shiraishi.junya@jaea.go.jp

Abstract:

Effects of plasma toroidal rotation are self-consistently taken into account not only in the magnetohydrodynamic (MHD) stability analysis but also in the equilibrium calculation. To study the effects of toroidal rotation on resistive wall modes (RWMs), a new code has been developed. The RWMaC modules, which solve the electromagnetic dynamics in vacuum and the resistive wall, have been implemented in the MINERVA code, which solves the Frieman-Rotenberg equation that describes the linear ideal MHD in a rotating plasma. It is shown for the first time that MHD equilibrium change induced by toroidal rotation significantly reduces the growth rates of RWMs. Moreover, it can open the stable window which does not exist under the assumption that the rotation affects only the linear dynamics. The rotation modifies the equilibrium pressure, current density, and mass density profiles, which results in the change of the potential energy including rotational effects.

1 Introduction

Unstable resistive wall modes (RWMs) limit the achievable beta value in high-beta steady-state tokamaks, and hence, they should be stabilized or controlled for operation of advanced tokamaks [1]. When the wall is sufficiently close to the plasma surface, it yields eddy currents to cancel the penetration of the magnetic field by unstable external kink mode. However, the eddy current decays in the time scale defined by the wall resistivity, which results in unstable RWMs. Theoretical [2] and experimental [3] researches have revealed that the plasma rotation is one of the most promising methods to stabilize RWMs. In rotating plasmas, there are many physical mechanisms that contribute to stabilization, e.g. the Alfvén or slow wave continuum damping and the kinetic resonance [4]. A linear ideal magnetohydrodynamics (MHD) code forms a basis for quantitative analysis of the above mechanisms. Conventional numerical codes [5, 6] introduce the plasma toroidal rotation as "perturbation," i.e., the rotation effect is not included in the equilibrium. In this study, the effect of MHD equilibrium change induced by toroidal rotation is investigated.

2 Generalized Grad-Shafranov equation

We consider MHD equilibria with toroidal rotation as $\boldsymbol{u}(R,Z) = R^2\Omega(\psi)\nabla\phi$ where (R-Z-ϕ) are the cylindrical coordinates, Ω is the plasma rotation frequency, and ψ is proportional to the poloidal magnetic flux. For axisymmetric equilibria ($\partial_\phi \equiv 0$), we obtain the "generalized" Grad-Shafranov equation (see, e.g. [7]) as

$$\Delta^*\psi = -F\frac{dF}{d\psi} - \mu_0 R^2 \left.\frac{\partial p}{\partial \psi}\right|_R, \quad \left.\frac{\partial p}{\partial R}\right|_\psi = \rho R \Omega^2, \tag{1}$$

where $\Delta^* = \partial_R^2 - R^{-1}\partial_R + \partial_Z^2$ is the Grad-Shafranov operator, $F = F(\psi)$ is proportional to the toroidal magnetic flux, μ_0 is the vacuum permeability, p is the pressure, and ρ is the mass density. Essential difference from the static Grad-Shafranov equation is attributed to the fact that the pressure is not a flux function but depends on R explicitly due to the centrifugal effect. By assuming the isothermal condition $T = T(\psi)$, the latter equation of (1) can be solved as

$$p(\psi, R) = p_0(\psi)\exp\left[M^2(\psi)\left(\frac{R^2}{R_0^2} - 1\right)\right], \tag{2}$$

where R_0 is the R coordinate of the magnetic axis, $M^2(\psi) = m_i R_0^2\Omega^2/(2T)$ is the squared Mach number with the ion mass m_i, and p_0 denotes the static pressure. Note that the mass density has the similar functional form.

We note that in the conventional numerical studies [5, 6], the effect of toroidal rotation on MHD equilibrium is neglected due to the smallness of M^2, i.e., $p \sim p_0(\psi)$. The rotational effects are "perturbative," i.e, they are introduced only in the linear dynamics. We call this equilibrium as "conventional" one. On the other hand, in this study, we incorporate the rotational effects self-consistently, i.e., we solve Eqs. (1) and (2), which is named "self-consistent equilibrium." We remark that in the self-consistent equilibria, the solution of ψ is modified, which results in the change of the pressure and the parallel current density, which play important roles in determining the MHD stability. These changes of equilibrium profiles affect the plasma potential energy, and are expected to change the property of the MHD stability.

3 Basic equations for linear dynamics of RWMs

3.1 Resistive wall and vacuum regions

We consider a plasma surrounded by an axisymmetric, poloidally-continuous wall. We call the vacuum region inside (outside) the wall "inner (outer) vacuum." Inner (outer) vacuum is denoted by IV (OV). The vacuum regions are governed by the pre-Maxwell equations, $\nabla \times \tilde{\boldsymbol{B}} = 0$ and $\nabla \cdot \tilde{\boldsymbol{B}} = 0$ where $\tilde{\boldsymbol{B}}$ is the perturbed magnetic field, which encourage us to introduce the magnetic scalar potential $\tilde{\boldsymbol{B}} = \nabla\chi^\pm$ in IV(OV). To represent the current flowing on the resistive wall, we introduce the current potential κ as $\tilde{\boldsymbol{J}} = \nabla s \times$

$\nabla\kappa(\theta,\phi,t)\delta(s-s_{\rm wall})$ where $\tilde{\boldsymbol{J}}$ is the perturbed current density, s (θ) is the appropriately-defined radial (poloidal) coordinate, $s_{\rm wall}$ is s at the wall, and δ is the Dirac's delta function. Integrating the Ampére's law across the wall, we get

$$\chi^{(w+)}(\theta,\phi,t)-\chi^{(w-)}(\theta,\phi,t)=\mu_0\kappa(\theta,\phi,t), \tag{3}$$

where the superscript (w) indicates the limit to the resistive wall. Integration of the Faraday's law and the Ohm's law on the resistive wall leads to

$$\frac{\Delta|\nabla s|}{\eta}\partial_t\tilde{B}^{(n)}=-\nabla\cdot\left(|\nabla s|^2\,\nabla_\perp\kappa\right), \tag{4}$$

where Δ is the wall width measured by s, η is the volume resistivity of the wall, $\nabla_\perp=\nabla-|\nabla s|^{-2}\nabla s(\nabla s\cdot\nabla)$, and $\tilde{B}^{(n)}=\tilde{\boldsymbol{B}}\cdot\hat{n}$ is the normal magnetic field with the unit normal $\hat{n}$.

We invoke eigenfunctions related to the eigenvalue problem on the wall, i.e, $-\nabla\cdot(|\nabla s|^2\nabla_\perp\kappa)=\omega|\nabla s|\kappa$. Solving this problem, we get an orthogonal set of eigenvalues and eigenfunctions as $\hat{\omega}_j$ and $\hat{\kappa}_j$. Then from Eq. (4), we can decompose the normal magnetic field and current potential on the wall as $B^{(n)}=\sum a_j(t)\hat{\kappa}_j(\theta,\phi)$ and $\kappa=(\Delta/\eta)\sum\hat{\omega}_j^{-1}\hat{\kappa}_j da_j/dt$ where a_j is the decomposition coefficient.

The quadratic form (energy balance) of Eq. (3) reads

$$\delta W_{IV}+\delta W_{OV}+\frac{1}{2\mu_0}\int_{S_p}\chi^{(p+)}\boldsymbol{Q}_e^*\cdot\hat{n}dS+\delta D_w=0, \tag{5}$$

where $\delta W_{IV(OV)}=1/(2\mu_0)\int_{IV(OV)}|\nabla\chi^\pm|^2 d\tau$ is the inner (outer) vacuum magnetic energy with the volume increment $d\tau$, $\delta D_w=(\Delta/2\eta)\sum\hat{\omega}_j^{-1}a_j^* da_j/dt$ is the energy dissipation in the resistive wall, and the asterisk indicates the complex conjugate. The third term of Eq. (5) indicates the plasma response where S_p is the plasma surface, the superscript (p) indicates the limit to S_p, and $\boldsymbol{Q}_e$ is the perturbed magnetic field on S_p.

3.2 Linear plasma response

We employ the Frieman-Rotenberg equation [8], which is the linearized ideal MHD equations with equilibrium rotation, as the governing equation in the plasma region,

$$\rho\partial_t^2\boldsymbol{\xi}+2\rho\left(\boldsymbol{u}\cdot\nabla\right)\partial_t\boldsymbol{\xi}=\mathcal{F}\boldsymbol{\xi}, \tag{6}$$

where $\boldsymbol{\xi}$ is the Lagrange displacement defined by $\tilde{\boldsymbol{u}}=:\partial_t\boldsymbol{\xi}+(\boldsymbol{u}\cdot\nabla)\boldsymbol{\xi}-(\boldsymbol{\xi}\cdot\nabla)\boldsymbol{u}$ where $\tilde{\boldsymbol{u}}$ is the perturbed rotation. The force operator $\mathcal{F}$ reads $\mathcal{F}\boldsymbol{\xi}=\mathcal{F}_s\boldsymbol{\xi}+\nabla\cdot[\rho\boldsymbol{\xi}(\boldsymbol{u}\cdot\nabla)\boldsymbol{u}-\rho\boldsymbol{u}(\boldsymbol{u}\cdot\nabla)\boldsymbol{\xi}]$ where $\mathcal{F}_s$ is similar to the conventional (static) force operator $\mathcal{F}_s\boldsymbol{\xi}=\nabla\left(\boldsymbol{\xi}\cdot\nabla p+\Gamma p\nabla\cdot\boldsymbol{\xi}\right)+\boldsymbol{J}\times\boldsymbol{Q}+\mu_0^{-1}(\nabla\times\boldsymbol{Q})\times\boldsymbol{B}$ with the equilibrium (perturbed) magnetic field $\boldsymbol{B}[\boldsymbol{Q}=\nabla\times(\boldsymbol{\xi}\times\boldsymbol{B})]$ and the ratio of specific heats $\Gamma=5/3$, however, it differs from the static one since $p=p(\psi,R)$ [see Eq. (2)]. We define the energy functional as $\delta K(\boldsymbol{\xi})=(1/2)\int\boldsymbol{\xi}^*\cdot\rho\partial_t^2\boldsymbol{\xi}d\tau$ (kinetic energy), $\delta W_c(\boldsymbol{\xi})=(1/2)\int\boldsymbol{\xi}^*\cdot\rho(\boldsymbol{u}\cdot\nabla)\partial_t\boldsymbol{\xi}d\tau$ (convective energy), and $\mathcal{V}(\boldsymbol{\xi})=-(1/2)\int\boldsymbol{\xi}^*\cdot\mathcal{F}\boldsymbol{\xi}d\tau$. The Frieman-Rotenberg equation reads

$\delta K + 2\delta W_c + \mathcal{V} = 0$. After some manipulation, we obtain $\mathcal{V} = \delta W_p + (1/2\mu_0)\int_{S_p}(\boldsymbol{Q}_e \cdot \boldsymbol{B}_e)\boldsymbol{\xi}^* \cdot \hat{n} dS$ where $\boldsymbol{B}_e$ is the equilibrium magnetic field on S_p. Note that the plasma potential energy includes the rotational effects as

$$\delta W_p \;=\; -\frac{1}{2}\int \left\{\boldsymbol{\xi}^* \cdot \mathcal{F}_s \boldsymbol{\xi} + \boldsymbol{\xi}^* \cdot \nabla \cdot \left[\rho \boldsymbol{\xi}\left(\boldsymbol{u}\cdot\nabla\right)\boldsymbol{u} - \rho \boldsymbol{u}\left(\boldsymbol{u}\cdot\nabla\right)\boldsymbol{\xi}\right]\right\} d\tau. \tag{7}$$

Substituting this plasma response $(1/2\mu_0)\int_{S_p}\chi^{(p+)}\boldsymbol{Q}_e^* \cdot \hat{n} dS = \delta K + 2\delta W_c + \delta W_p$ into Eq. (5), we get the energy balance in the plasma-wall-vacuum system as

$$\delta K + 2\delta W_c + \delta W_p + \delta W_{IV} + \delta W_{OV} + \delta D_w = 0. \tag{8}$$

To solve Eq.(8), we have developed "RWMaC" modules to compute the vacuum magnetic energy $\delta W_{IV(OV)}$ and the energy dissipation δD_w by solving the pre-Maxwell equations in vacuum and the eigenvalue problem in the resistive wall. The remaining plasma energy terms, i.e., δK, δW_c, and δW_p are computed by the MINERVA code [9]. MINERVA solves the Frieman-Rotenberg equation (6) in tokamak geometry as an initial value problem as well as a boundary value problem. MINERVA/RWMaC has been benchmarked with NMA code [10] without rotation and with MARS-F [11] with toroidal rotation by using the conventional equilibrium.

4 RWM stabilization in self-consistent equilibria

We focus on the RWMs in self-consistent equilibria to include the equilibrium change induced by toroidal rotation. Note that the conventional numerical studies [5, 6] neglect the rotation in the equilibrium. We consider three cases of high-β_N ($\beta_N = 3.4, 4.2, 5.53$) equilibria with fixing the D-shape of plasma surface (the ellipticity $\kappa = 1.91$ and the triangularity $\delta = 0.50$), the toroidal magnetic field at the magnetic axis $B_0 = 1.7$T, and plasma current $I_p = 2.3$MA, which are typical parameters for advanced plasma designed for JT-60SA [12]. As shown in Fig. 1, the β_N value is changed by scaling the pressure with keeping the almost same safety factor and current density profiles.

The profile of toroidal rotation frequency is characterized by $\Omega(\psi) = \Omega_0[1-(\psi/\psi_a)^2]^2$ where Ω_0 is the rotation frequency at the magnetic axis ψ_a is the ψ at the plasma surface. As shown in Fig. 2, by changing Ω_0 and fixing the mass density, we consider two case of rotation frequency characterized by its frequency at the $q = 3$ surface as $\Omega|_{q=3} = 0.02\omega_A$ and $0.04\omega_A$ where ω_A is the Alfvén frequency defined by toroidal magnetic field at the magnetic axis. Note that this rotation frequency range is relevant to low-aspect ratio tokamaks.

Figure 3 shows MINERVA/RWMaC computation of the growth rates of RWM without rotation, RWM in conventional equilibria, and RWM in self-consistent equilibria as functions of the wall position for each equilibrium with two rotation amplitude. We have used the toroidal mode number $n = 1$ and $\tau_w/\tau_A = 3 \times 10^3$ where $\tau_w = \mu_0 bd/\eta$ is the wall decay time with the wall width (radius) d (b) and τ_A is the Alfvén transit time at the magnetic axis. As shown in Fig. 3, in the self-consistent equilibria, the RWM growth rate is reduced in the wide range of wall position. Some results ($\beta_N = 3.4$ and $\beta_N = 4.2$ with $\Omega|_{q=3} = 0.04\omega_A$) indicates that the self-consistent equilibrium has an extended stable window compared with the conventional case. It is seen that the stable window shifts toward the plasma surface. Another results ($\beta_N = 3.4$ with $\Omega|_{q=3} = 0.02\omega_A$ and $\beta_N = 5.53$ with $\Omega|_{q=3} = 0.04\omega_A$) show that the self-consistent equilibrium has the stable window even if there is no window in conventional equilibrium. These results verify that in general, for the toroidal rotation with $\Omega/\omega_A = O(1\%)$, the growth rates of RWMs are significantly reduced in the self-consistent equilibrium.

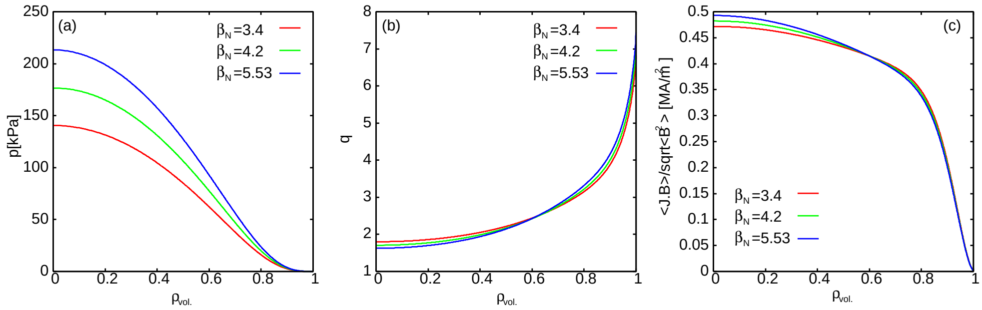

FIG. 1: Equilibrium profiles as functions of plasma volume for some β_N values, $\beta_N = 3.4, 4.2, 5.53$. (a) Pressure (b) Safety factor (c) Parallel current.

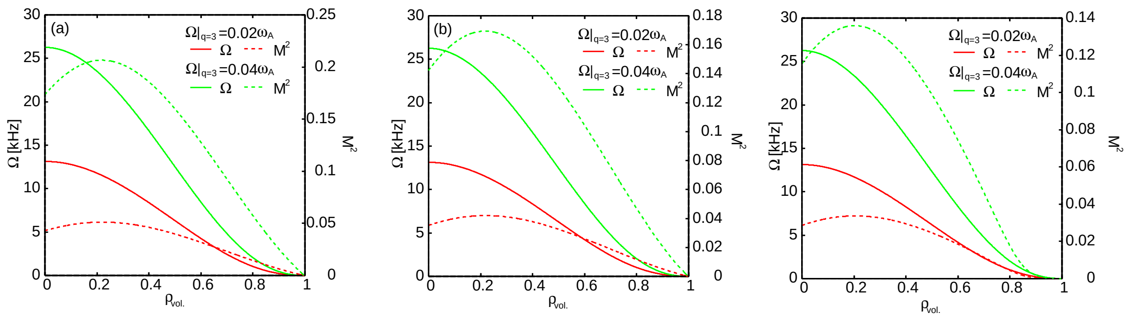

FIG. 2: Rotation frequency (solid lines) and squared Mach (dashed lines) number profiles as functions of plasma volume for some β_N values, (a) $\beta_N = 3.4$ (b) $\beta_N = 4.2$ (c) $\beta_N = 5.53$.

5 Analysis of energy balance

To investigate the mechanism of RWM stabilization in the self-consistent equilibria, we study the energy balance (8) to clarify which energy source/sink term significantly affects the RWM stablity. When the RWM is eigenmode as in the present case, we can assume that the perturbation is written as $\propto \exp(\lambda t)$ thus we can put $\partial_t \equiv \lambda$ where λ is a

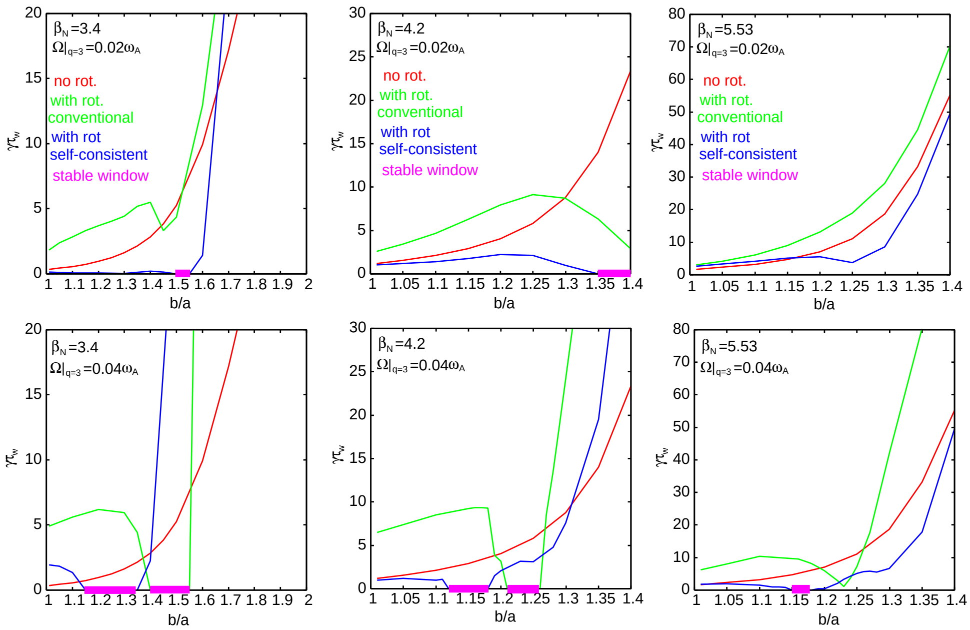

FIG. 3: Normalized growth rates of RWMs without rotation, RWMs with rotation but without equilibrium change, and RWMs with equilibrium change vs. wall position for $\beta_N = 3.4$, 4.2, and 5.53 with rotation frequencies $\Omega|_{q=3} = 0.02\omega_A$ and $0.04\omega_A$.

complex eigenvalue. Since the growth rate and the real frequency for RWM are sufficiently small, we can safely neglect the inertia term $\lambda^2\delta K$, which yields a dispersion relation, $\lambda = -(\delta W_p + \delta W_{IV} + \delta W_{OV})/(\delta D_w + 2\delta W_c)$. Since δW_p, $\delta W_{IV(OV)}$, and δD_w are real (Hermite) and δW_c is pure imaginary (anti-Hermite), the RWM growth rate is determined as

$$\gamma = \Re(\lambda) = -\frac{\delta W_p + \delta W_{IV} + \delta W_{OV}}{|\delta D_w + 2\delta W_c|^2}\delta D_w. \tag{9}$$

Note that $\delta W_{IV(OV)}$ and δD_w are positive definite. The RWM stability is determined by the sign of $\delta W_p + \delta W_{IV} + \delta W_{OV}$, and the growth rate is scaled by $\delta D_w/|\delta D_w + 2\delta W_c|^2$.

The plasma potential energy δW_p, Eq. (7), can be decomposed [13] as

$$\delta W_p = \delta W_s + \delta W_d + \delta W_{rot}, \tag{10}$$

where δW_s is the Hermitiam part of $(1/2)\int \boldsymbol{\xi}^* \cdot \mathcal{F}_s\boldsymbol{\xi} d\tau$, $\delta W_{rot} = (1/2)\int \rho\boldsymbol{\xi}^* \cdot (\boldsymbol{u}\cdot\nabla)(\boldsymbol{u}\cdot\nabla)\boldsymbol{\xi} d\tau$ denotes the destabilizing centrifugal energy induced by plasma rotation, and δW_d is the dynamic part, which works to sustain the Hermicity of δW_p.

We employ a typical computation result with $\beta_N = 4.2$ and $\Omega|_{q=3} = 0.02\omega_A$, which clearly shows that the RWM growth rates are reduced in the self-consistent equilibrium. Note that the energy balance behaves in a similar way at the left side of the stable window (if exists) for all the equilibria studied in the previous section. Figure 4 shows the each energy term normalized by $\delta D_w/|\delta D_w + 2\delta W_c|^2$ as a function of wall location for $b/a < 1.3$.

The essential difference between two cases is attributed to the behavior of δW_s, δW_{rot}, and $\delta W_{IV} + \delta W_{OV}$. Note that the dynamic part δW_d is small compared with the centrifugal part δW_{rot}, which always destabilizes RWMs. In the conventional equilibrium, δW_s works as stabilizing and destabilizing energy compatible with the vacuum magnetic energy. On the other hand, in the self-consistent equilibrium, δW_s is always stabilizing and is much stronger than the vacuum contribution. As is shown in Fig. 4 , the energy balance of the RWM stability is drastically changed when the effect of toroidal rotation is included in the equilibrium calculation.

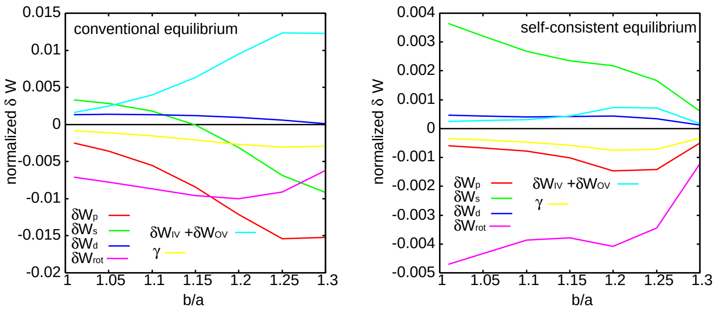

FIG. 4: Plot of energy source/sink in the dispersion relation (9) and (10) as functions of wall location (b/a $<$ 1.3) for $\beta_N = 4.3$ and $\Omega|_{q=3} = 0.02\omega_A$ for conventional and self-consistent equilibria. The plasma potential energy δW_p is decomposed into Hermite part δW_s, dynamic part δW_d, and centrifugal part δW_{rot}. All energies are normalized by $\delta D_w/|\delta D_w + 2\delta W_c|^2$.

6 Summary

Summarizing, to study how the effects of toroidal rotation that modifies MHD equilibrium, we have developed RWMaC modules that solves electromagnetic problems in vacuum and the resistive wall, and implemented RWMaC modules in the linear ideal MHD code with equilibrium rotation MINERVA. We have benchmarked MINERVA/RWMaC with NMA code (without rotation) and MARS-F code (with rotation).

By using MINERVA/RWMaC, we have investigated the RWMs in MHD equilibria that self-consistently includes the effects of toroidal rotation with different β_N values and rotation frequencies. We have showed that in general, the RWM growth rates are reduced in the self-consistent MHD equilibria. Moreover, the self-consistent equilibrium can have the stable window even if there is no window for conventional equilibrium. These results indicate that the MHD equilibrium should include rotational modification when analyzing the experimental data with modest plasma rotation frequency. By analyzing the energy balance, we have shown that the energy balance in the plasma-wall-vacuum system is drastically changed when the rotation effect is included in the equilibrium. As for conventional equilibria, the Hermite part of the potential energy δW_s and centrifugal energy δW_{rot} balance with the vacuum magnetic energy, and determine the RWM stability.

On the other hand, for self-consistent equilibrium, the δW_s is dominant over the vacuum contribution, and determines the RWM growth rate by balancing with δW_{rot}.

The authors are grateful to Dr. M. Mori, Dr. Y. Kamada, and Dr. T. Ozeki for their support. JS thanks Dr. M.S. Chu and Dr. L.L. Lao for their benchmarking efforts. This work was supported by KAKENHI 24760708.

References

[1] CHU, M.S. and OKABAYASHI, M., "Stabilization of the external kink and the resistive wall mode", Plasma Phys. Control. Fusion 52 (2010) 123001.

[2] BONDESON, A. and WARD, D.J., "Stabilization of external modes in tokamaks by resistive walls and plasma rotation", Phys. Rev. Lett. 72 (1994) 2709.

[3] TAKECHI, M, et al., "Identification of a Low Plasma-Rotation Threshold for Stabilization of the Resistive Wall Mode", Phys. Rev.. Lett. 98 (2007) 055002.

[4] HU, B. and BETTI, R., "Resistive Wall Mode in Collisionless Quasistationary Plasmas", Phys. Rev. Lett. 93 (2004) 105002.

[5] LIU, Y. et al., "Progress in physics and control of the resistive wall mode in advanced tokamaks", Phys. Plasmas 16 (2009) 056113.

[6] BERKERY, J.W. et al., Phys. Rev. Lett. 104 (2010) 035003.

[7] PUSTOVITOV, V.D., Plasma Phys. Rep. 29 (2003) 124.

[8] FRIEMAN, E. and ROTENBERG, M., "On Hydromagnetic Stability of Stationary Equilibria", Phys. Rev. Lett. 32 (1960) 898.

[9] AIBA, N. et al., "MINERVA: Ideal MHD stability code for toroidally rotating tokamak plasmas", Comput. Phys. Commun. 180 (2009) 1282.

[10] CHU, M.S. et al., "Normal mode approach to modeling of feedback stabilization of the resistive wall mode", Nucl. Fusion 43 (2003) 441.

[11] CHU, M.S. et al., "Effect of toroidal plasma flow and flow shear on global magnetohydrodynamic MHD modes", Phys. Plasmas 2 (1995) 2236.

[12] ISHIDA, S. et al., "Overview of the JT-60SA project", Nucl. Fusion 52 (2011) 094018.

[13] AIBA, N. et al., "Destabilization mechanism of edge localized MHD mode by a toroidal rotation in tokamaks", Nucl. Fusion 50 (2010) 045002.